

Formation of hypernuclei in relativistic ion collisions

Alexander Botvina

FIAS, Goethe University, Frankfurt am Main (Germany) ,
Institute for Nuclear Research, RAS, Moscow (Russia)

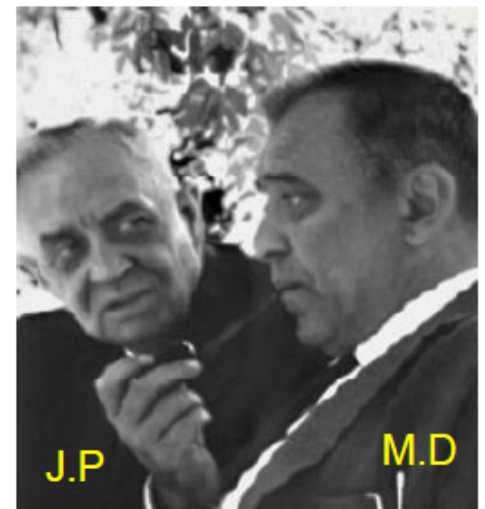
(collaboration with M.Bleicher, J.Steinheimer,
J.Pochodzalla, N.Buyukcizmeci, K.K.Gudima)

**NuSPRASEN Workshop on Nuclear Reactions (ENSAR2) ,
*Warsaw, Poland.***

January 22-24 , 2018

Discovery of a Strange nucleus: Hypernucleus

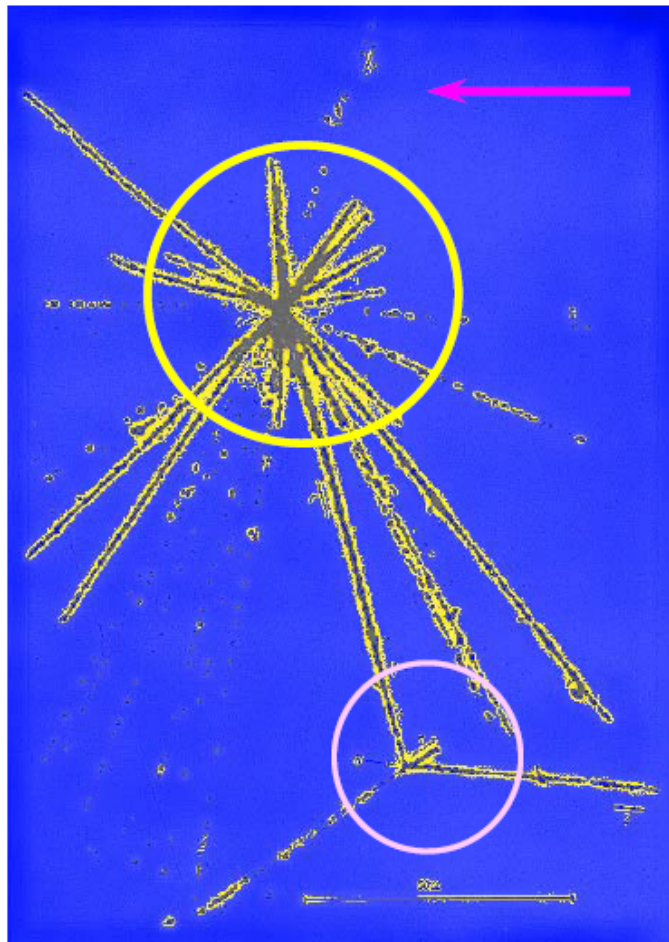
M. Danysz and J. Pniewski, *Philos. Mag.* 44 (1953) 348



J.P

M.D

First-hypernucleus was observed in a stack of photographic emulsions exposed to cosmic rays at about 26 km above the ground.



Incoming high energy proton from cosmic ray

colliding with a nucleus of the emulsion, breaks it in several fragments forming a star. **Multifragmentation !**

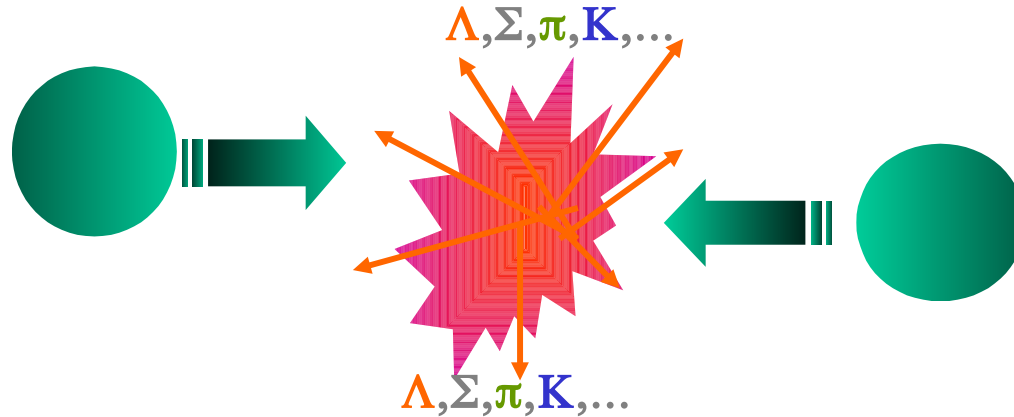
All nuclear fragments stop in the emulsion after a short path

From the first star, 21 Tracks $\Rightarrow 9\alpha + 11\text{H} + 1_{\Lambda}\text{X}$

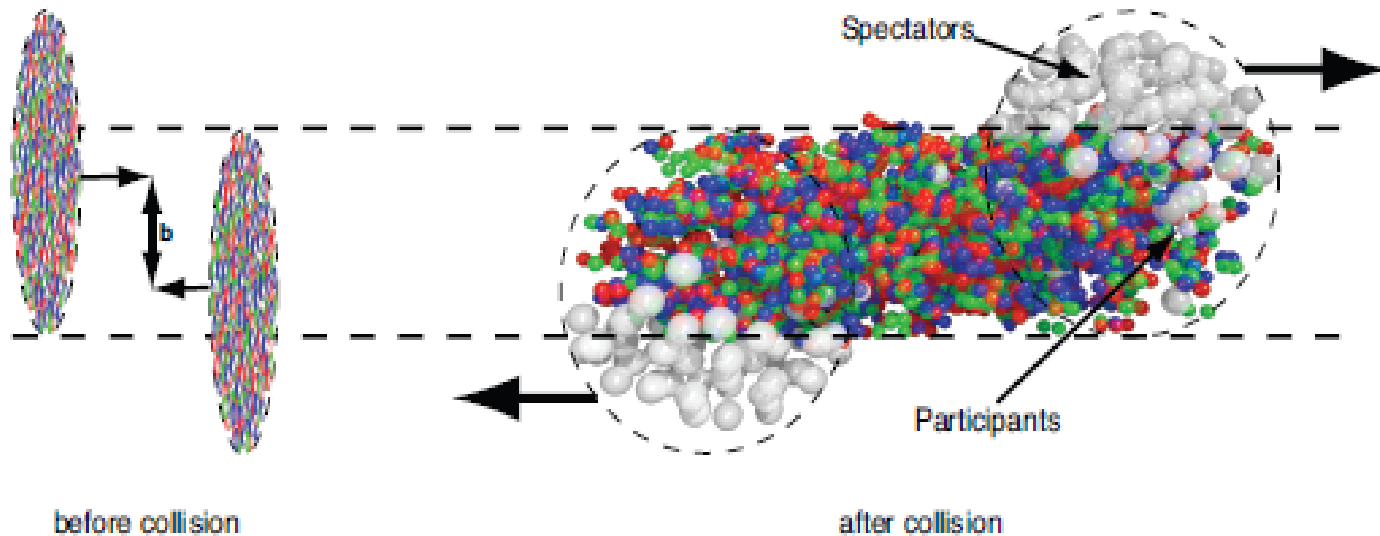
The fragment $_{\Lambda}\text{X}$ disintegrates later, makes the bottom star. Time taken $\sim 10^{-12}$ sec (typical for weak decay)

This particular nuclear fragment, and the others obtained afterwards in similar conditions, were called **hyperfragments or hypernuclei**.

Relativistic collisions of hadrons and ions



Production of hypernuclei in central and peripheral HI collisions



UrQMD

PHSD

DCM

GiBUU

Production of hypermatter in HI and hadron collisions:

- Production of strange particles and hyperons by “participants”,
- Secondary production and rescattering of hyperons,
- Coalescence of hyperons and baryons,
- Capture of produced baryons by excited “spectators”.

Statistical decay of excited hypermatter into hypernuclei

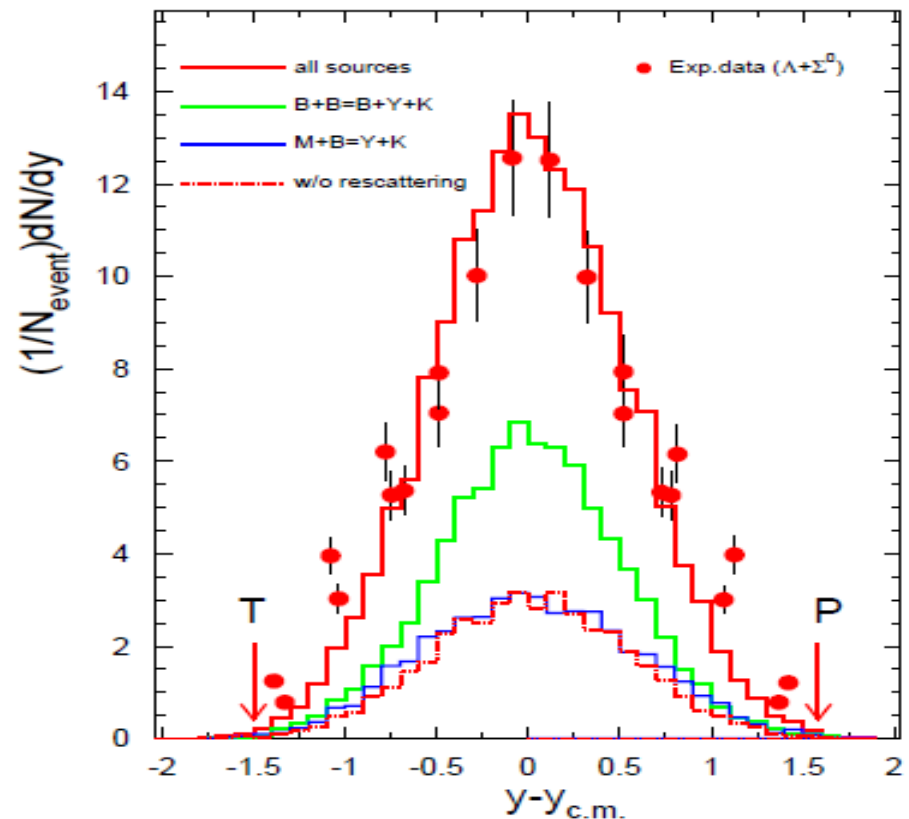
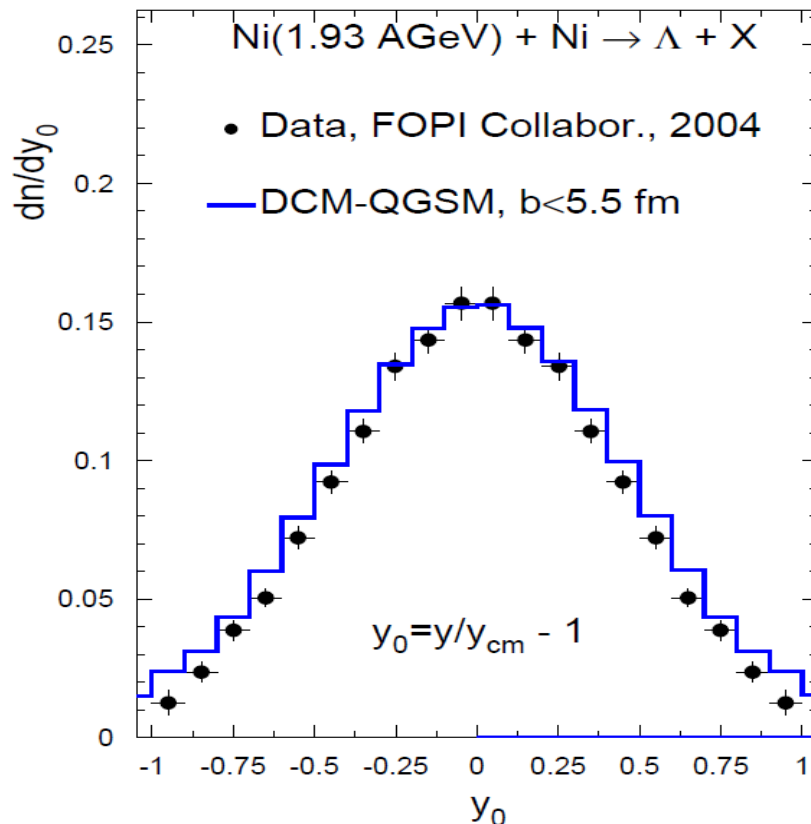
- Multifragmentation into small nuclei (high excitations),
- Evaporation and fission of large nuclei (low excitations),
- (Fermi-) Break-up of small nuclei into lightest ones.

Peripheral collisions. All transport modes predict similar picture:
Hyperons can be produced can be produced at all rapidities, in
participant and spectator kinematic regions.

Wide rapidity distribution of
produced Λ !

Calculation: DCM
PRC84(2011)064904
Au(11A GeV/c)+Au

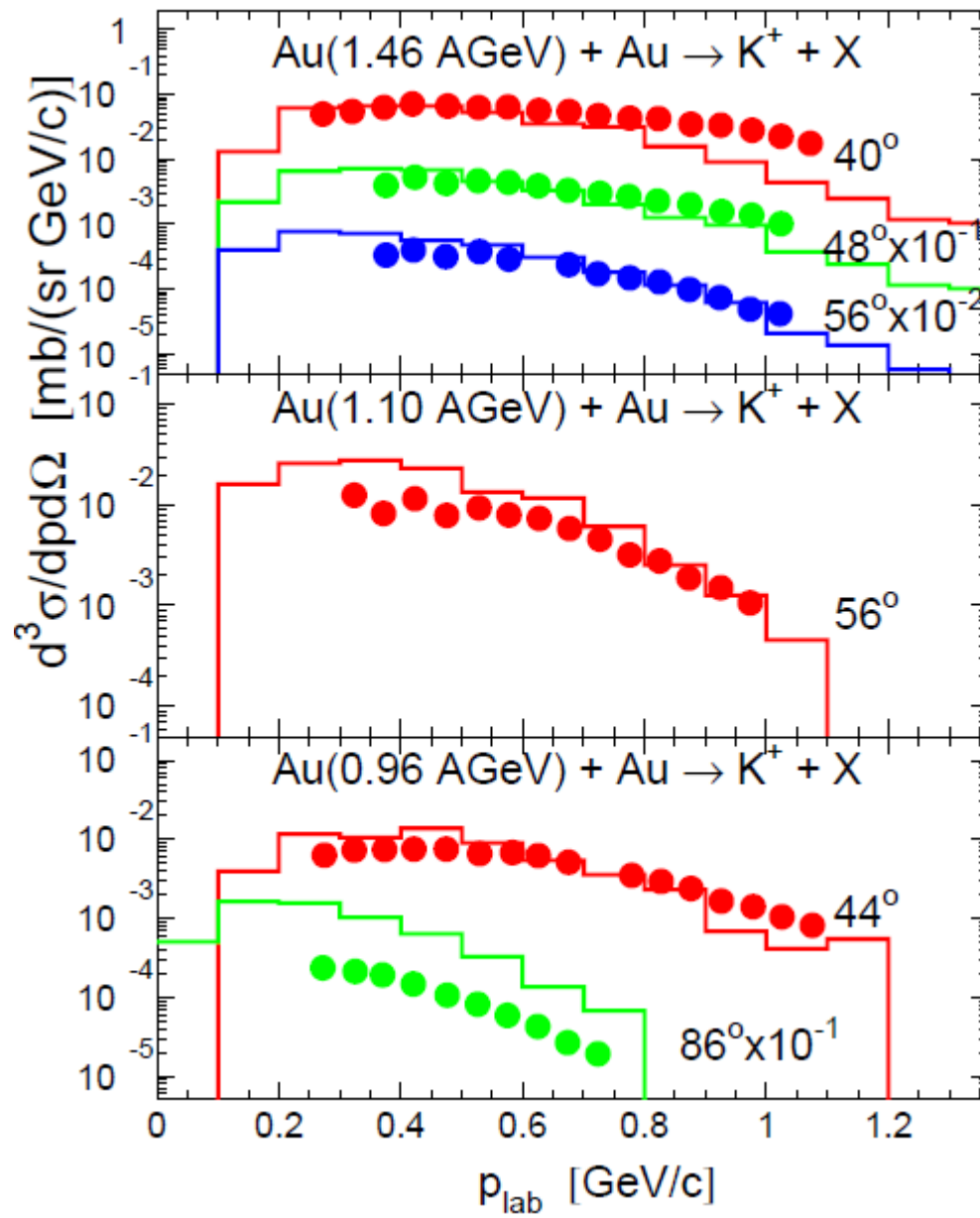
S.Albergo et al.,
E896:
PRL88(2002)062301



Dominating: $p+n \rightarrow n+\Lambda+K^+$, $\pi+p \rightarrow \Lambda+K^+$

DCM

Comparison with KAOS data
Phys. Rev. C75 (2007) 02490



Coalescence of Baryons (CB) Model :

Development of the coalescence for formation of clusters of all sizes

- 1) Relative velocities between baryons and clusters are considered,
if $(|\mathbf{V}_b - \mathbf{V}_A|) < V_c$ the particle b is included in the A-cluster.
- 2) Step by step numerical approximation.
- 3) In addition, coordinates of baryons and clusters are considered,
if $|\mathbf{X}_b - \mathbf{X}_A| < R * A^{1/3}$ the particle b may be included in A-cluster.
- 4) Spectators' nucleons are always included in the residues.

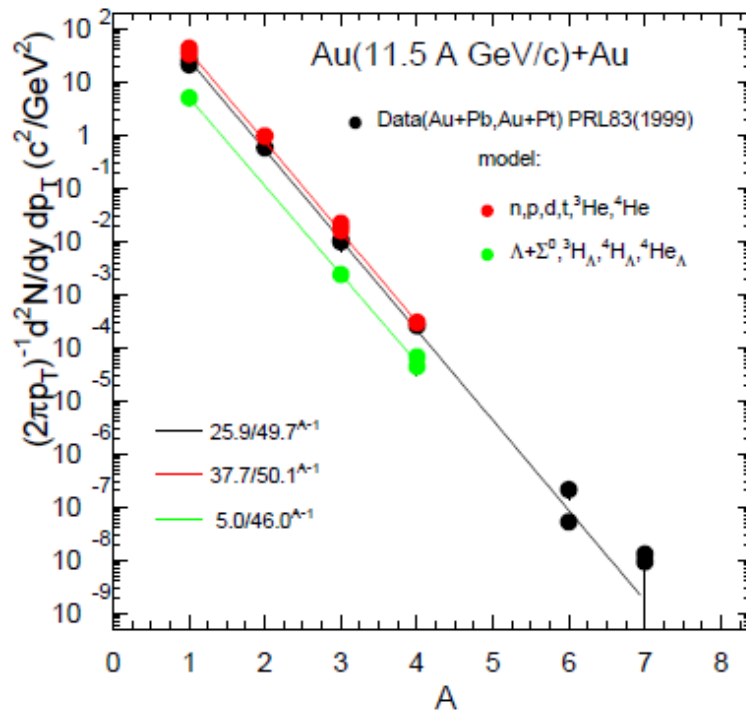
Combination of transport UrQMD and HSD models with CB:

Investigation of fragments/hyperfragments at all rapidities !
(connection between central and peripheral zones)

Production of light nuclei in central collisions :

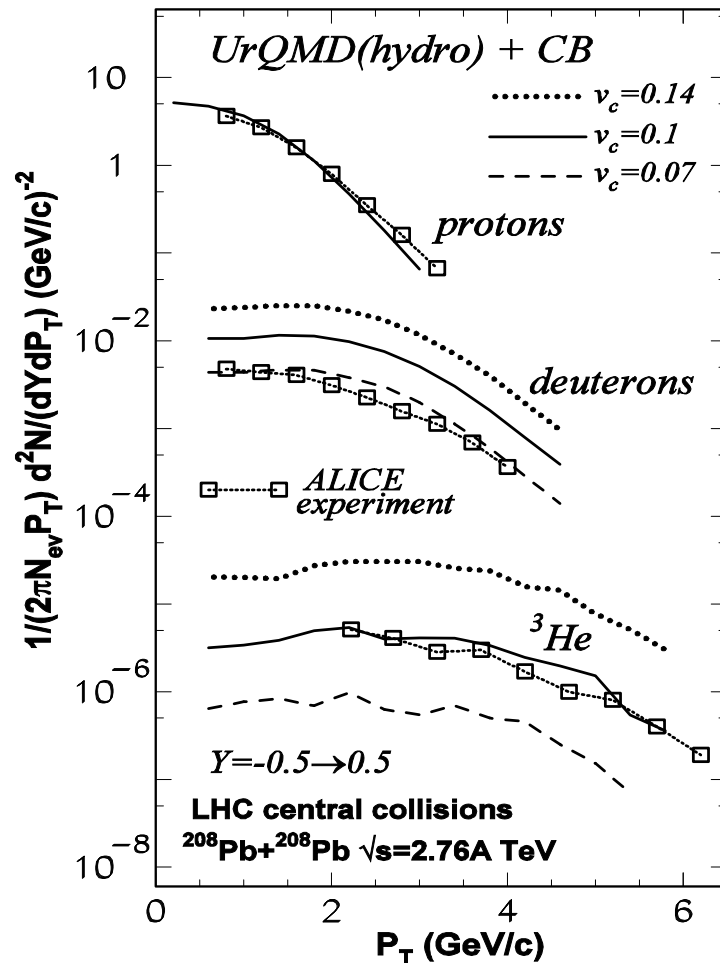
DCM, UrQMD, CB - Phys. Lett. B714, 85 (2012), Phys. Lett. B742, 7 (2015)

DCM versus experiment :
coalescence mechanism

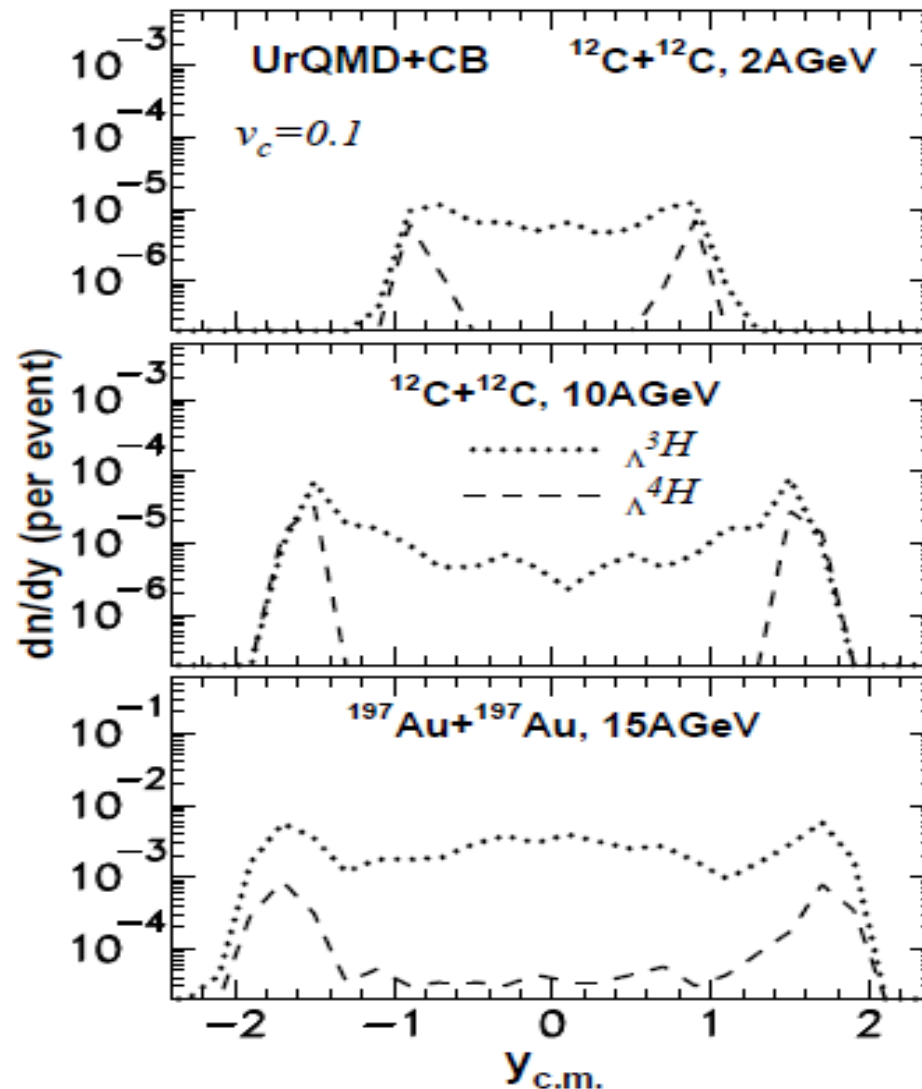


It is not possible to
produce big nuclei !

Hybrid approach at LHC energies:
UrQMD+hydrodynamics+coalescence



Because of secondary interactions the maximum of the fragments production is shifted from the midrapidity. Secondary products have relatively low kinetic energies, therefore, they can produce clusters and hypernuclei with higher probability.

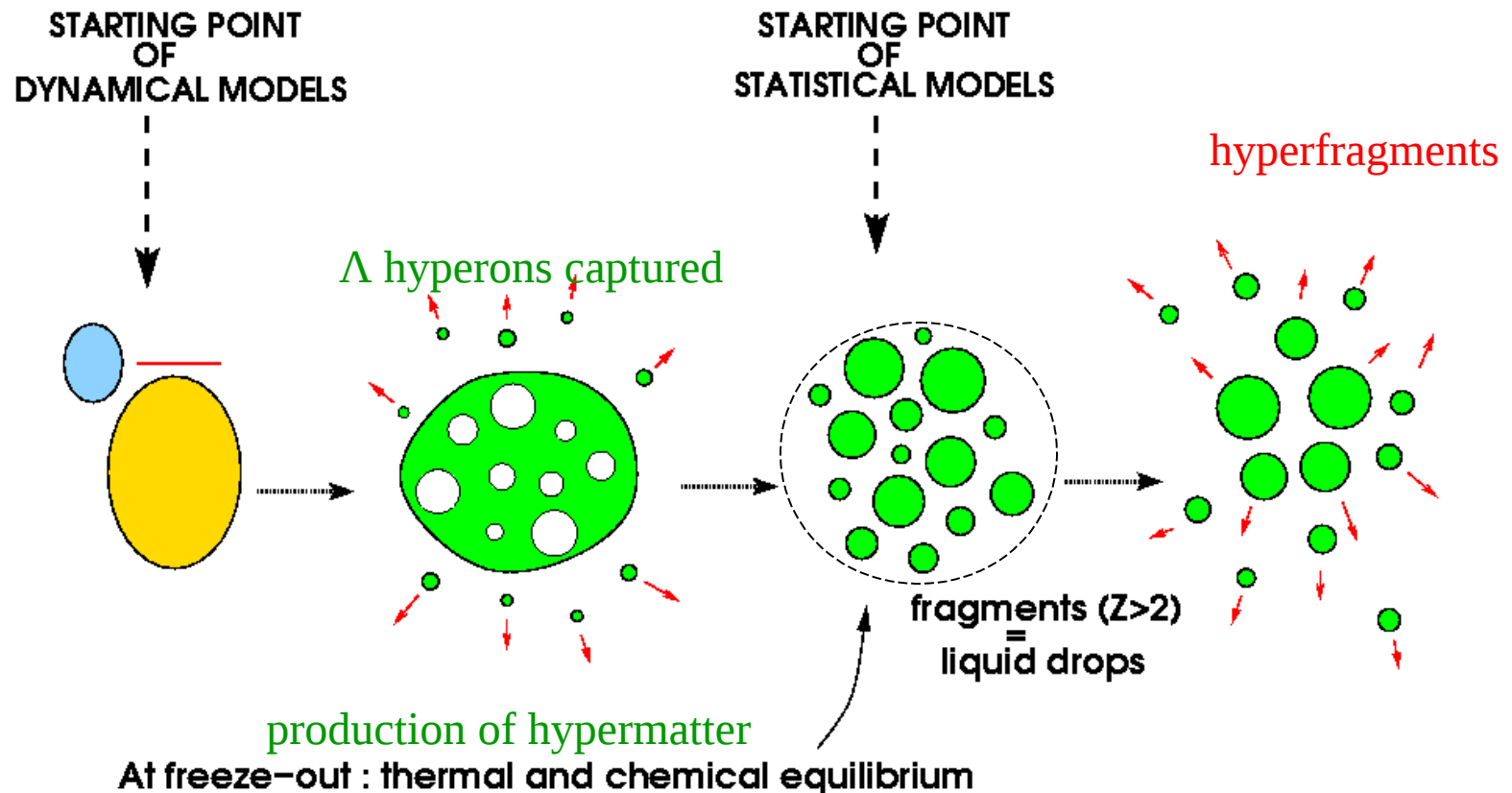


A.S.Botvina and J.Pochodzalla, Phys. Rev.C76 (2007) 024909

Generalization of the statistical de-excitation model for nuclei with Lambda hyperons

In these reactions we expect analogy with
multifragmentation in intermediate and high energy nuclear reactions

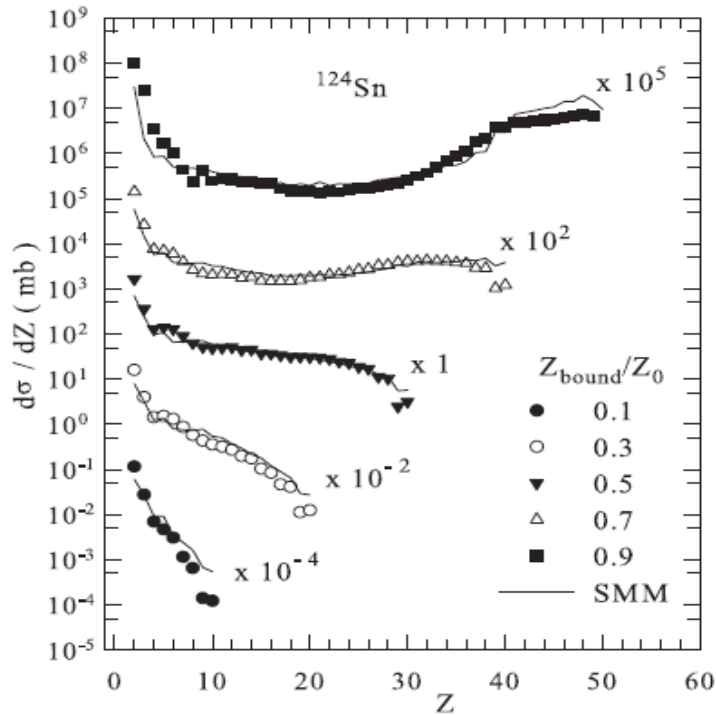
+ nuclear matter with strangeness



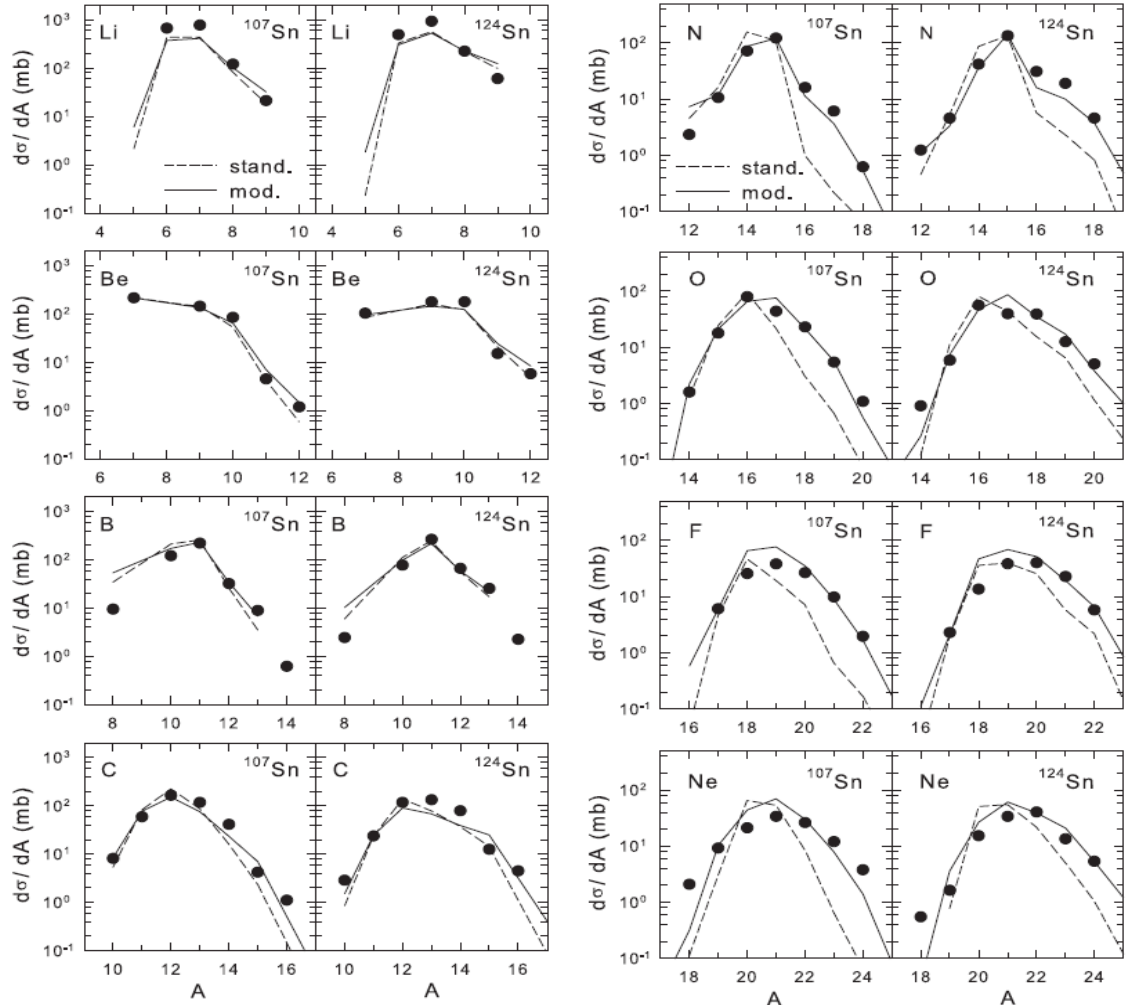
Isospin-dependent multifragmentation of relativistic projectiles

$^{124,107}\text{Sn}$, ^{124}La (600 A MeV) + Sn \rightarrow projectile (multi-)fragmentation

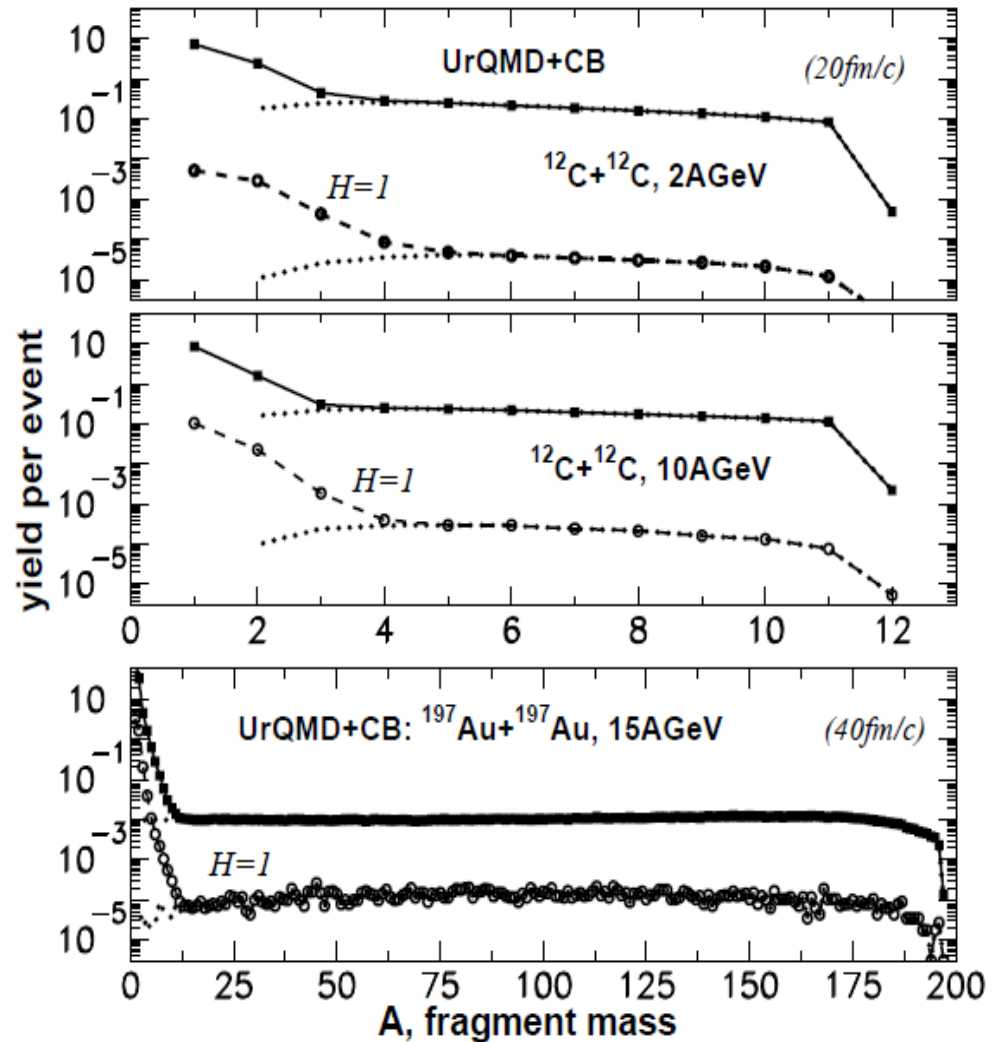
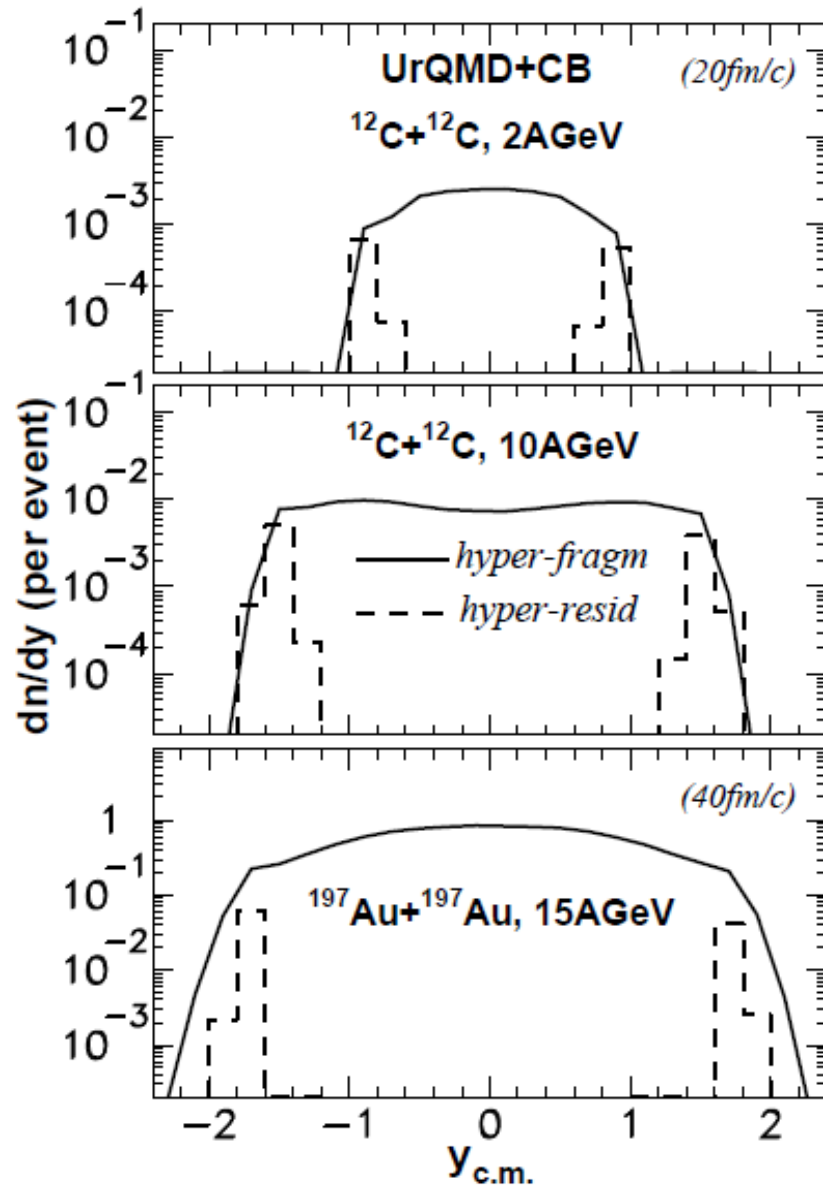
Very good description is obtained within Statistical Multifragmentation Model, including fragment charge yields, isotope yields, various fragment correlations.



Statistical (chemical) equilibrium is established at break-up of hot projectile residues ! In the case of strangeness admixture we expect it too !

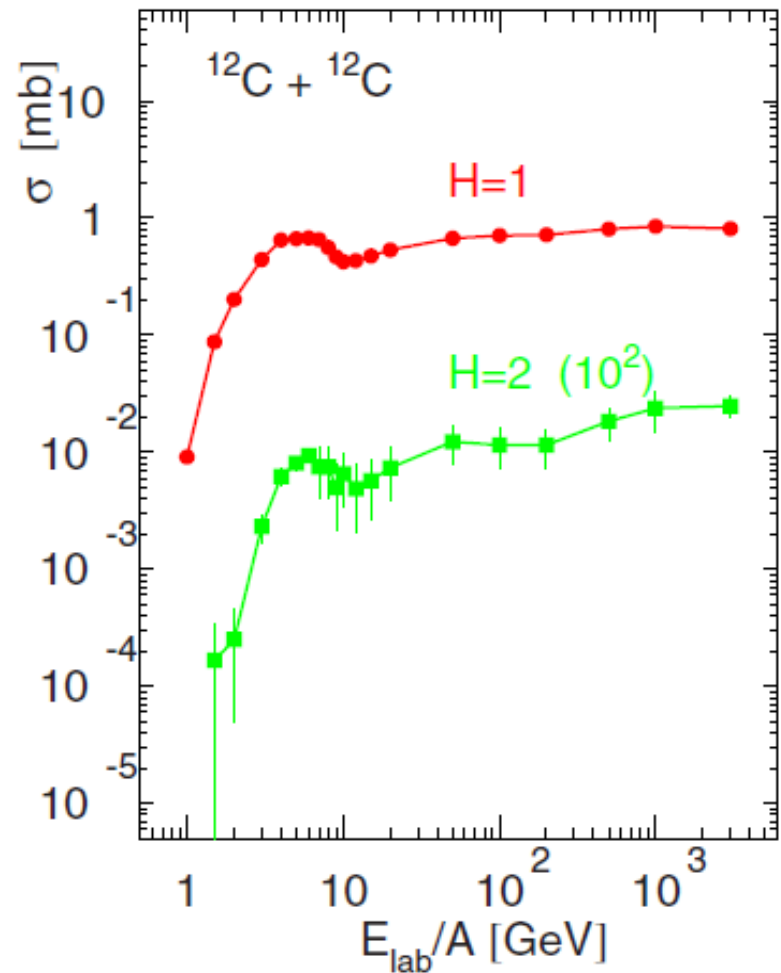
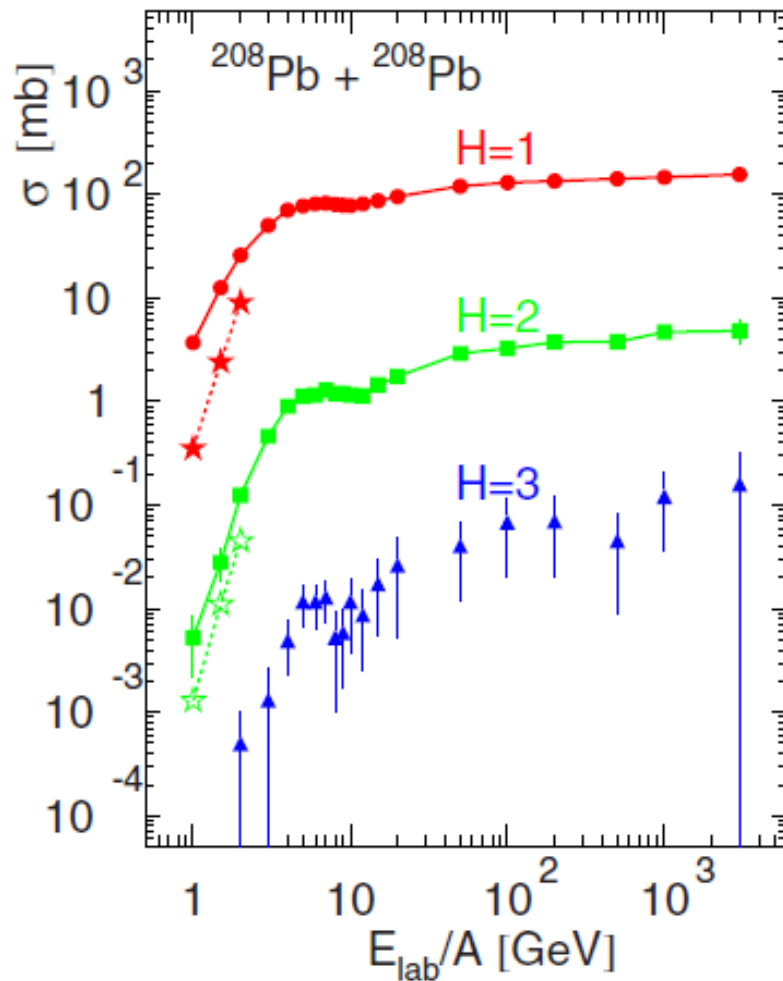


normal- and hyper-fragments; hyper-residues @ target/projectile rapidities



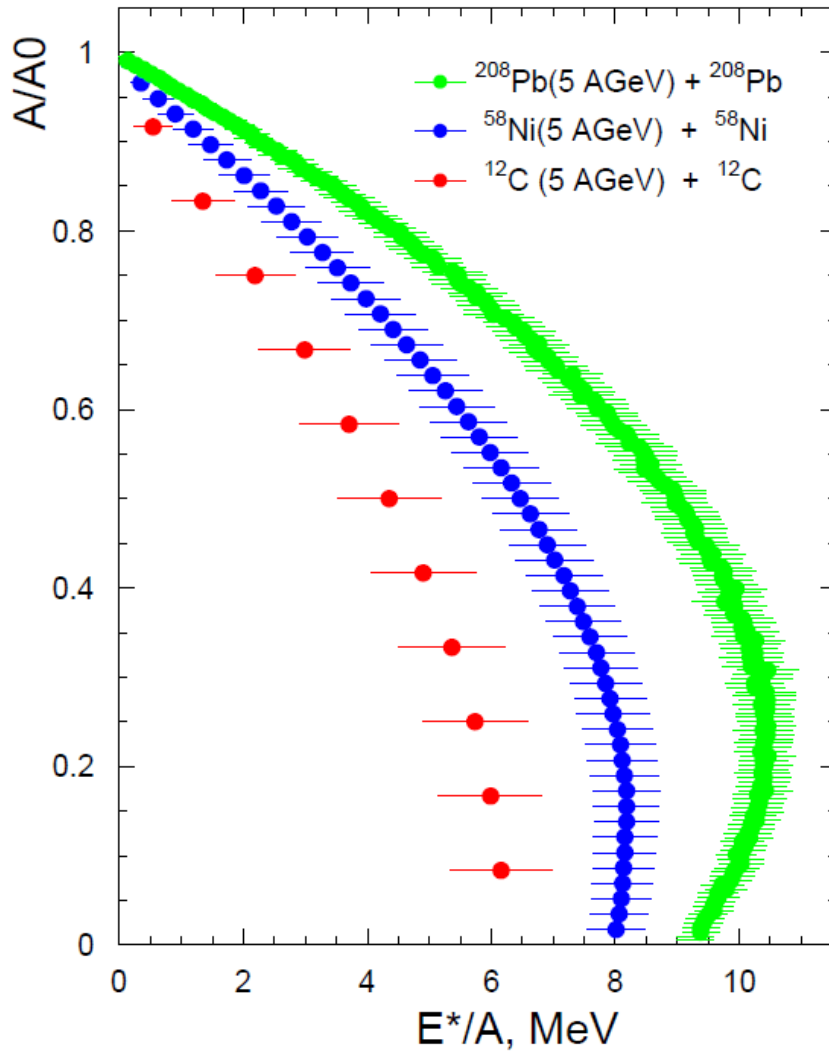
Production of excited hyper-residues in peripheral collisions, decaying into hypernuclei (target/projectile rapidity region).

DCM and UrQMD + CB predictions: Phys. Rev. C95, 014902 (2017)



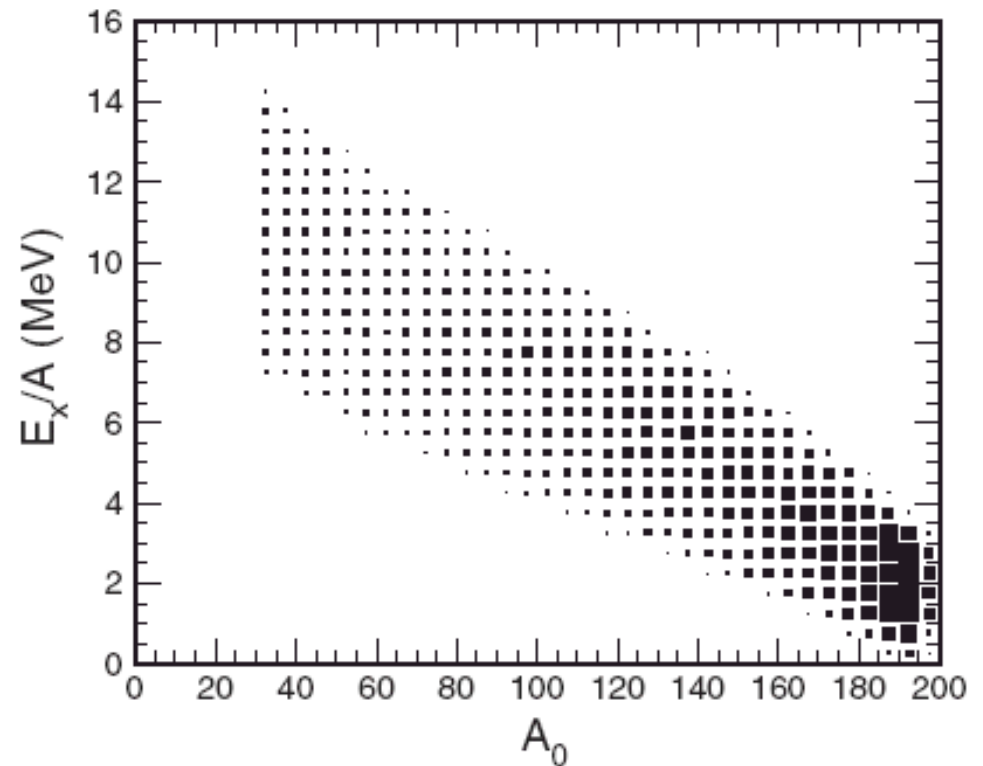
Excitation energies of the residual nuclei

DCM



ALADIN analysis: Au+Au at 1 A GeV data (GSI)

H.Xi et al.,
Z.Phys. A359(1997)397



4.3.3. Evaporation from hot fragments

The successive particle emission from hot primary fragments with $A > 16$ is assumed to be their basic de-excitation mechanism. Due to the high excitation energy of these fragments, the standard Weisskopf evaporation scheme [2] was modified to take into account the heavier ejectiles up to ^{18}O , besides light particles (nucleons, d , t , α), in ground and particle-stable excited states [81]. This corresponds to the excitation energies $\epsilon^{(i)}$ of the ejectiles not higher than 7–8 MeV. By analogy with standard model the width for the emission of a particle j from the compound nucleus (A, Z) is given by:

$$\Gamma_j = \sum_{i=1}^n \int_0^{E_{AZ}^* - B_j - \epsilon_j^{(i)}} \frac{\mu_j g_j^{(i)}}{\pi^2 \hbar^3} \sigma_j(E) \frac{\rho_{A'Z'}(E_{AZ}^* - B_j - E)}{\rho_{AZ}(E_{AZ}^*)} E dE \quad (60)$$

Here the sum is taken over the ground and all particle-stable excited states $\epsilon_j^{(i)}$ ($i = 0, 1, \dots, n$) of the fragment j , $g_j^{(i)} = (2s_j^{(i)} + 1)$ is the spin degeneracy factor of the i th excited state, μ_j and B_j are corresponding reduced mass and separation energy, E_{AZ}^* is the excitation energy of the initial nucleus (55), E is the kinetic energy of an emitted particle in the centre-of-mass frame. In Eq. (60) ρ_{AZ} and $\rho_{A'Z'}$ are the level densities of the initial (A, Z) and final (A', Z') compound nuclei. They are calculated using the Fermi-gas formula (41). The cross section $\sigma_j(E)$ of the inverse reaction $(A', Z') + j = (A, Z)$ was calculated using the optical model with nucleus–nucleus potential from Ref. [117]. The evaporational process was simulated by the Monte Carlo method using the algorithm described in Ref. [118]. The conservation of energy and momentum was strictly controlled in each emission step.

Evaporation from hypernuclei: nucleons, light particles, hyperons, light hypernuclei:
New masses and assuming the level densities as in normal nuclei.

4.3.4. Nuclear fission

An important channel of de-excitation of heavy nuclei ($A > 200$) is fission. This process competes with particle emission. Following the Bohr–Wheeler statistical approach we assume that the partial width for the compound nucleus fission is proportional to the level density at the saddle point $\rho_{sp}(E)$ [1]:

$$\Gamma_f = \frac{1}{2\pi\rho_{AZ}(E_{AZ}^*)} \int_0^{E_{AZ}^* - B_f} \rho_{sp}(E_{AZ}^* - B_f - E) dE, \quad (61)$$

where B_f is the height of the fission barrier which is determined by the Myers–Swiatecki prescription [120]. For approximation of ρ_{sp} we used the results of the extensive analysis of nuclear fissility and Γ_n/Γ_f branching ratios [121]. The influence of the shell structure on the level densities ρ_{sp} and ρ_{AZ} is disregarded since in the case of multifragmentation we are dealing with very high excitation energies $E^* > 30\text{--}50$ MeV when shell effects are expected to be washed out [122].

Fission of hypernuclei: New fission barriers including hyperon interaction (in the liquid-drop approach). It leads to increasing the barriers for ~ 1 MeV.

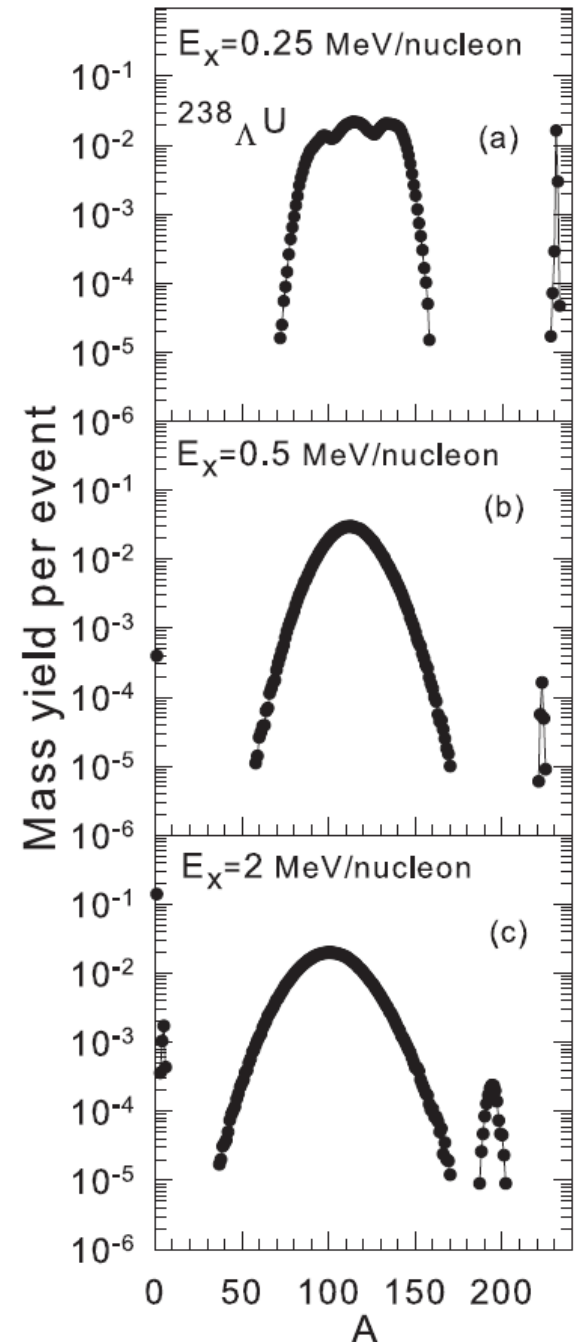
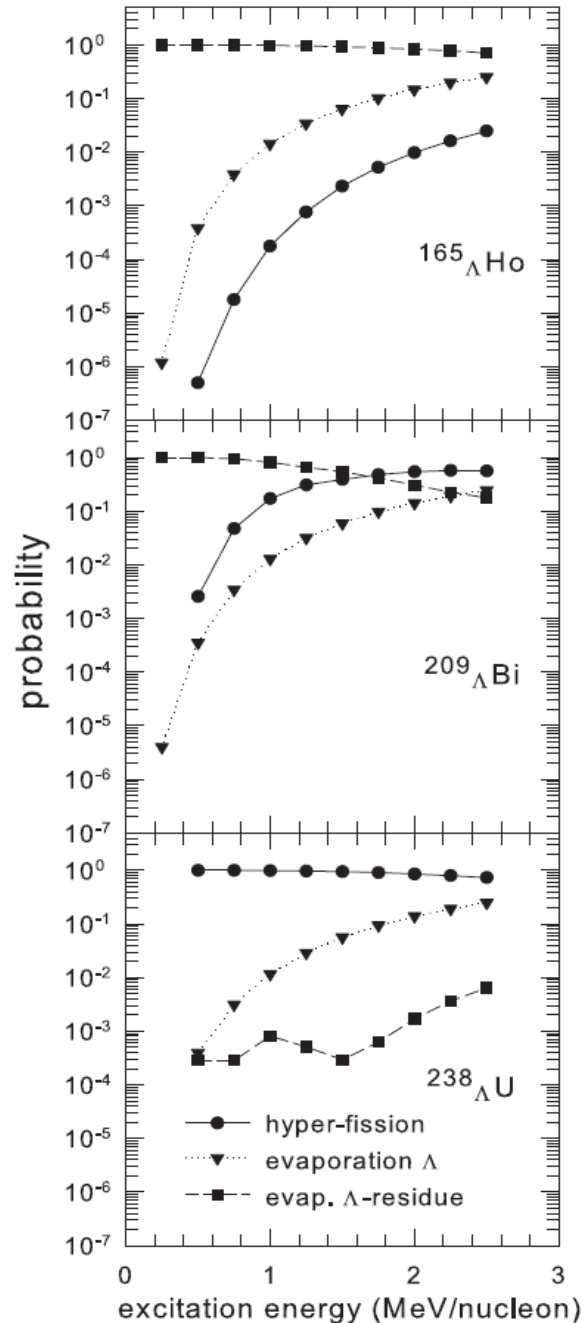
The level densities at the saddle point are taken as in normal nuclei (first approximation).

Evaporation & Fission of hypernuclei

(depending on mass and
excitation energy)

A.S.Botvina et al.,
Phys. Rev. C94
(2016) 054615

These processes recall
normal fission and
evaporation. However,
producing exotic hyper-
fragments is possible
(e.g. neutron rich ones)
to investigate hyperon
interactions in astro-
physical conditions.



Statistical approach for fragmentation of hyper-matter

$$Y_{AZH} = g_{AZH} V_f \frac{A^{3/2}}{\lambda_T^3} \exp \left[-\frac{1}{T} (F_{AZH} - \mu_{AZH}) \right]$$

$\mu_{AZH} = A\mu + Z\nu + H\xi$

mean yield of fragments with mass number A , charge Z , and Λ -hyperon number H

$$F_{AZH}(T, V) = F_A^B + F_A^S + F_{AZH}^{\text{sym}} + F_{AZ}^C + F_{AH}^{\text{hyp}}$$

liquid-drop description of fragments: bulk, surface, symmetry, Coulomb (as in Wigner-Seitz approximation), and hyper energy contributions
J.Bondorf et al., Phys. Rep. **257** (1995) 133

$$F_A^B(T) = \left(-w_0 - \frac{T^2}{\varepsilon_0} \right) A \quad ,$$

$$F_A^S(T) = \beta_0 \left(\frac{T_c^2 - T^2}{T_c^2 + T^2} \right)^{5/4} A^{2/3} \quad ,$$

parameters \approx Bethe-Weizsäcker formula:
 $w_0 = 16 \text{ MeV}, \beta_0 = 18 \text{ MeV}, T_c = 18 \text{ MeV}$

$$F_{AZH}^{\text{sym}} = \gamma \frac{(A - H - 2Z)^2}{A - H} \quad , \quad \gamma = 25 \text{ MeV} \quad [\varepsilon_0 \approx 16 \text{ MeV}]$$

$$\sum_{AZH} A Y_{AZH} = A_0, \quad \sum_{AZH} Z Y_{AZH} = Z_0, \quad \sum_{AZH} H Y_{AZH} = H_0.$$

chemical potentials are from mass, charge and Hyperon number conservations

$$F_{AH}^{\text{hyp}} = E_{sam}^{\text{hyp}} = H \cdot (-10.68 + 48.7/(A^{2/3})).$$

-- C.Samanta et al. J. Phys. G: 32 (2006) 363 (motivated: single Λ in potential well)

$$F_{AH}^{\text{hyp}} = (H/A) \cdot (-10.68A + 21.27A^{2/3}).$$

-- liquid-drop description of hyper-matter

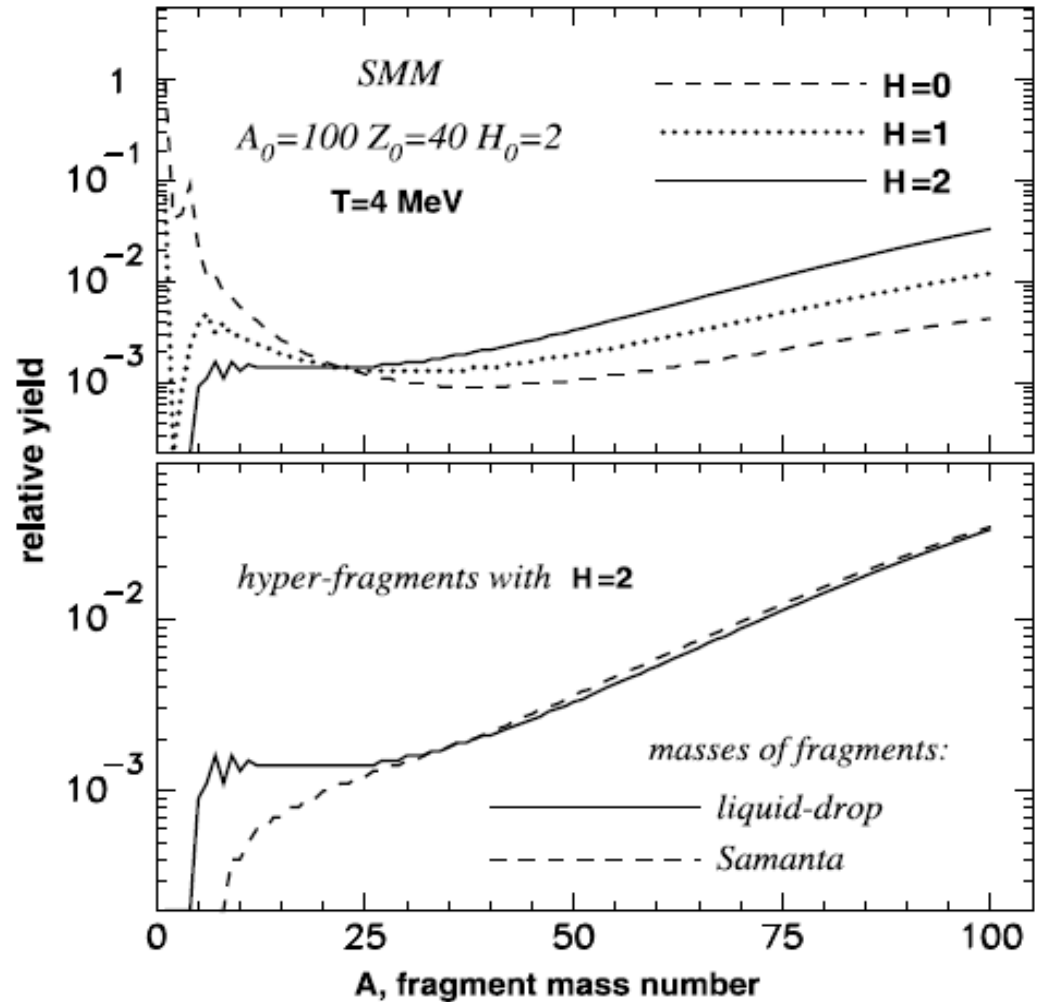
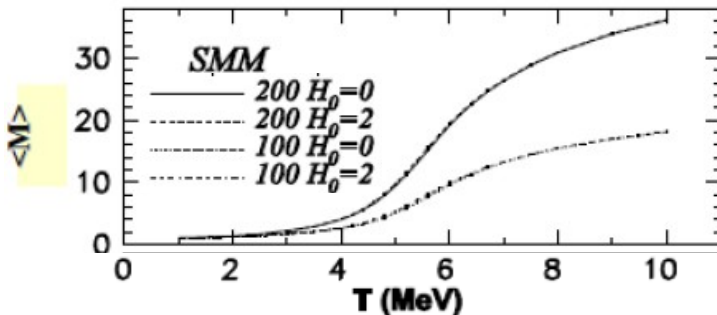
A.S.Botvina and J.Pochodzalla, Phys. Rev.C76 (2007) 024909

Multifragmentation of excited hyper-sources

H_0 is the number of hyperons in the system in the system

General picture depends weakly on strangeness content (in the case it is much lower than baryon charge)

Mean multiplicity



However, there are essential differences in properties of produced fragments !

Fig. 3. Multifragmentation of an excited double-strange system with mass number 100 and charge 40, at temperature 4 MeV. Top panel – yield of fragments containing 0, 1, and 2 Λ hyperons. Bottom panel – effect of different mass formulae with strangeness on production of double hyperfragments [13].

De-excitation of hot light hypernuclear systems

A.Sanchez-Lorente, A.S.Botvina, J.Pochodzalla, Phys. Lett. B697 (2011)222

For light primary fragments (with $A \leq 16$) even a relatively small excitation energy may be comparable with their total binding energy. In this case we assume that the principal mechanism of de-excitation is the explosive decay of the excited nucleus into several smaller clusters (the secondary break-up). To describe this process we use the famous Fermi model [105]. It is analogous to the above-described statistical model, but all final-state fragments are assumed to be in their ground or low excited states. In this case the statistical weight of the channel containing n particles with masses m_i ($i = 1, \dots, n$) in volume V_f may be calculated in microcanonical approximation:

$$\Delta \Gamma_f^{\text{mic}} \propto \frac{S}{G} \left(\frac{V_f}{(2\pi\hbar)^3} \right)^{n-1} \left(\frac{\prod_{i=1}^n m_i}{m_0} \right)^{3/2} \frac{(2\pi)^{(3/2)(n-1)}}{\Gamma(\frac{3}{2}(n-1))} (E_{\text{kin}} - U_f^C)^{(3/2)n-5/2}, \quad (58)$$

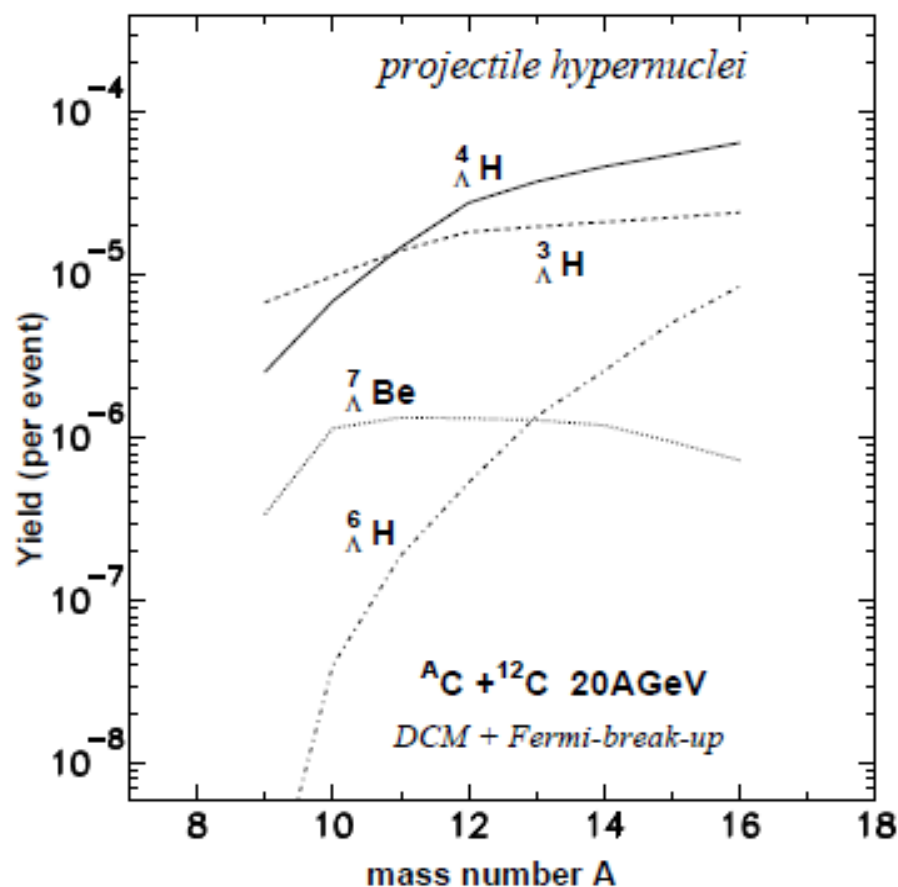
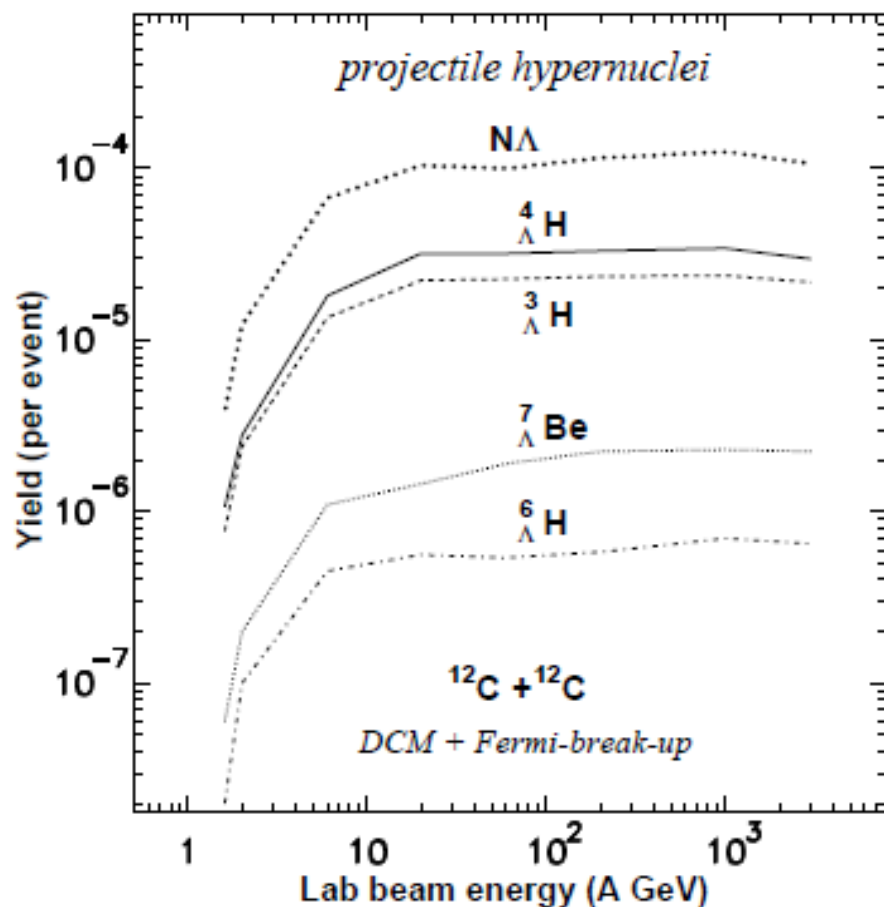
where $m_0 = \sum_{i=1}^n m_i$ is the mass of the decaying nucleus, $S = \prod_{i=1}^n (2s_i + 1)$ is the spin degeneracy factor (s_i is the i th particle spin), $G = \prod_{j=1}^k n_j!$ is the particle identity factor (n_j is the number of particles of kind j). E_{kin} is the total kinetic energy of particles at infinity which is related to the prefragment excitation energy E_{AZ}^* as

$$E_{\text{kin}} = E_{AZ}^* + m_0 c^2 - \sum_{i=1}^n m_i c^2. \quad (59)$$

U_f^C is the Coulomb interaction energy between cold secondary fragments given by Eq. (49), U_f^C and V_f are attributed now to the secondary break-up configuration.

Generalization of the Fermi-break-up model: new decay channels with hypernuclei were included ; masses and spins of hypernuclei and their excited states were taken from available experimental data and theoretical calculations

Production of light hypernuclei in relativistic ion collisions



One can use exotic neutron-rich and neutron-poor projectiles, which are not possible to use as targets in traditional hyper-nuclear experiments, because of their short lifetime. Comparing yields of hypernuclei from various sources we can get info about their binding energies and properties of hyper-matter.

Conclusions

Collisions of relativistic ions and hadrons with nuclei are promising reactions for novel research of hypernuclei, anti-nuclei, and exotic nuclei. These processes are theoretically confirmed with various models.

Mechanisms of formation of hypernuclei in peripheral reactions: Strange baryons (Λ , Σ , Ξ , ...) produced in particle collisions can be transported to the spectator residues and captured in nuclear matter. Another mechanism is the coalescence of baryons leading to light clusters, including anti-matter, will be effective at all rapidities. These exotic systems are presumably excited and after their decay novel hypernuclei of all sizes (and isospin), including exotic weakly-bound states, multi-strange nuclei, anti-nuclei can be produced.

Advantages over other reactions: in the spectator matter there is no limit on sizes and isotope content of produced exotic nuclei; probability of their formation may be high; a large strangeness can be deposited in nuclei.

Correlations (unbound states) and lifetimes can be naturally studied.

EOS of hypermatter at subnuclear density and hyperon interactions in exotic nuclear matter can be investigated.